Ouahiba Bouriche*, Brahim Bouzerafa and Hicham Kouadri

Electrochemical, optical and morphological properties of poly (N-vinylcarbazole/TiO_2) and (N-vinylcarbazole/aniline)/TiO_2 copolymer prepared by electrochemical polymerization

https://doi.org/10.1515/epoly-2017-0105
Received May 31, 2017; accepted July 19, 2017

Abstract: Poly (N-vinylcarbazole) (PVK) and a new copolymer, PVK/polyaniline (PANI), have been successfully prepared by electrochemical polymerization of N-vinylcarbazole (NVK) and NVK/aniline from acetonitrile medium and $LiClO_4$ supporting electrolyte. Composite thin films were studied by cyclic voltammetry (CV) in $LiClO_4$/acetonitrile solutions on an indium tin oxide (ITO) electrode. The influences of concentration of titanium dioxide (TiO_2) on the electrochemical properties of these composite materials were also investigated. The results of scanning electron microscopy (SEM) confirm the presence of TiO_2 in the composite, which consequently modifies the morphology of the film significantly. Topographical analysis has shown that TiO_2 nanoparticles (NPs) affect the morphology of thin films (roughness). The analysis of the voltammograms of PVK and of (PVK+PANI) before and after the addition of TiO_2 at different concentrations shows a redox couple which was not observed in the absence of TiO_2. The impedance spectroscopy study shows that the resistance of the PVK and (PVK+PANI) films decreases with increasing of TiO_2 concentration, and this in turn contributes to a good conductivity of the film. The optical characterization of the composites has been carried out by UV-Vis absorption and photoluminescence (PL) spectroscopy and it was noted that the samples (PVK+10^{-2} TiO_2) exhibited high transmittance (83%) in the visible region and a low gap value (2.69 eV) which confirms that this material can be used in a photovoltaic cell. This is explained by the introduction of the donor levels in the band gap of PVK by the TiO_2, due to an effective doping.

Keywords: composite; cyclic voltammetry; electropolymerization; ITO; NVK; PANI; poly (N-vinylcarbazole); titanium dioxide.

1 Introduction

Poly (N-vinylcarbazole) (PVK) has outstanding physicochemical properties (photoconductive, photo-refractive, high refractive index) and it is used in many areas which are currently booming: photovoltaic cell, holograms photocopies (1–4). To date, the exploitation of PVK as an active material component has occurred mainly with doped PVK or PVK blends (5–7). Many methods such as the bath deposition method, sol-gel process, spray pyrolysis and electrochemical deposition have been used to prepare PVK. This latter is much used due to its various advantages such as its simplicity, low cost, low temperature process, deposition on large and complex areas and capability to control material properties and morphology by different electrochemical parameters. Lacaze et al. (8) studied the electrochemical oxidation of N-vinylcarbazole (NVK) in CH_3CN on a transparent tin oxide. The results indicate that poly (NVK) films endowed with electro chromic properties can be formed electrochemically on transparent semiconductor surfaces [indium tin oxide (ITO)]. Patrice et al. (9) studied the electrochemical doping of PVK films which were electrochemically prepared in ($LiClO_4$ 0.5 M)/CH_3CN. Baibarac et al. (10) also studied electrochemical polymerization of NVK and carbon nanotubes by cyclic voltammetry (CV) in $LiClO_4$/acetonitrile. The influence of monomer concentration and supporting electrolytes on the polymerization conditions and electrochemical properties of these composite materials were investigated.

Semiconductor NPs have properties different from those of bulk materials and are attractive materials that hold considerable potential for numerous applications in the fields of electronics and photonics (11). Titanium

***Corresponding author: Ouahiba Bouriche,** Laboratory: Preparation and Modification of Multiphase Polymeric Materials (LMPMP), Department of Process Engineering, University of Ferhat Abbas Setif 1, Setif 19000, Algeria; and Center of Scientific and Technical Research in Physicochemical Analyzes, Tipaza Algeria 384, Industrial Zone Bou_Ismail RP, 42004 Tipaza, Algeria, Tel.: +213.549.99.36.82, e-mail: anesk2011@yahoo.fr; anesines@yahoo.fr
Brahim Bouzerafa: Laboratory: Preparation and Modification of Multiphase Polymeric Materials (LMPMP), Department of Process Engineering, University of Ferhat Abbas Setif 1, Setif 19000, Algeria
Hicham Kouadri: Laboratory: Preparation and Modification of Multiphase Polymeric Materials (LMPMP), Department of Process Engineering, University of Ferhat Abbas Setif 1, Setif 19000, Algeria; and Center of Scientific and Technical Research in Physicochemical Analyzes, Tipaza Algeria 384, Industrial Zone Bou_Ismail RP, 42004 Tipaza, Algeria

Brought to you by | University of Gothenburg
Authenticated
Download Date | 10/14/17 8:04 AM

dioxide (TiO_2) on the nanometer scale has been widely studied as a semiconductor substrate for dye-sensitized solar cells (12–15).

Much research has been done on the composite of PVK/TiO_2 NPs. Cho et al. (16) used TiO_2 NPs embedded in poly(9-vinylcarbazole) (PVK) film, and Ramar et al. (17) prepared hybrid nanocomposites TiO_2/PVK by simple blending of TiO_2 with small quantities of PVK (0.3–1.3 wt%) in the presence of PEG. Sonone et al. (18) used the bath deposition method for the fabrication of polymeric thin films of PVK with nano-crystalline TiO_2.

Polyaniline (PANI), and its composites, has been widely investigated owing to its ease of protonic acid doping in the emeraldine form and to its environmental stability in both doped and undoped forms. In addition, PANIs are relatively lightweight and corrosion-resistant conducting materials, and may be easily produced at large scale at a low cost (19). PANI is among the most studied conducting polymers found in a variety of applications such as rechargeable batteries, photonics, optoelectronic devices, biochemical sensing devices, membrane separation as well as modified electrodes for electro-reduction (20). Also, PANI/TiO_2 nanocomposite has attracted more attention in recent years (21–24).

In the study we have carried out, special attention is given to the TiO_2 functionalized with poly(NVK/PANI) to evaluate its possible use in optoelectronic and photonic devices.

In this work, PVK and a new copolymer (PANI + PVK) were synthesized, and the TiO_2 effect on the electrochemical, structural hybrid film, optical band gap and photoluminescence (PL) properties was studied. CV and impedance spectroscopy measurements were used to get information on electrochemical properties and spectroscopic characterization of composite materials obtained from PVK, PANI and TiO_2. The optical characterization of the composites has been carried out by UV-Vis transmittance and PL spectroscopy, while the morphological properties have been investigated by atomic force microscopy (AFM) and scanning electron microscopy (SEM).

2 Experimental

2.1 Materials

Aniline and NVK with 99.99% purity as monomer (Aldrich product, USA), TiO_2 99.9% (Aldrich, USA), powder at different concentrations of: 0, 10^{-2} M; $3 \cdot 10^{-2}$ M; $5 \cdot 10^{-2}$ M as a doping semiconductor. The supporting electrolyte used in electropolymerization is lithium perchlorate ($LiClO_4$ 0.1 M) (Fluka product, Switzerland) dissolved in acetonitrile (CH_3CN).

2.2 Preparation of composite films

The composite films deposited on ITO were carried out in a glass cell obtained by CV, containing the [solution + NVK ($6 \cdot 10^{-3}$ M)], or solution + [An (0.1 M) + NVK ($6 \cdot 10^{-3}$ M)] or the same composition + TiO_2 at v = 10 mV/s, between −0.8 and 1.8 V/SCE in which three electrodes are immerged. The working electrode is an ITO (SOLEMS) prior to the deposition process, the ITO substrates were ultrasonically cleaned in methanol, acetone and distillate water for 10 min and etched in H_2SO_4 45% for 2 min to activate the surface of the electrode, which was fixed at 1 cm^2 area. The reference electrode is a saturated calomel electrode with KCl (SCE) and the auxiliary electrode is platinum.

2.3 Instrumental analysis

Electrochemical impedance spectroscopy (EIS) measurements were performed using an alternative current voltage of 10 mV, at open circuit potential (Eocp), in the frequency range 50 KHz and 100 MHz.

The surface morphology of PVK, PVK/TiO_2, (PVK + PANI), (PVK + PANI)/TiO_2 films was characterized by atomic force spectroscopy (AFM) (USA) and SEM (USA). PL (Perkin Elmer LS 50B) spectroscopy and a Shimadzu UV-Visible spectrometer (Japan) were used to investigate the optical properties of the composites, PL measurements proceeded on thin films by exciting the samples with 325 nm (3.81 eV) line of a 150 W Xenon lamp. All measurements were performed at room temperature.

3 Results and discussion

3.1 Electropolymerization of NVK in CH_3CN medium

Figure 1A and B shows the voltammograms recorded in the presence of $LiClO_4$ (0.1 M) and NVK ($3 \cdot 10^{-6}$ M), between −0.8 and 1.8 V/SCE. The oxidation of NVK starts at 0.8 V/SCE and, on the backsweep, gives rise to a reduction wave at 0.95 V (cycle 1). These waves can be ascribed to the electrochemical behavior of carbazoles, or to the formation and reduction of the carbazolylium cation radical (8–10). The increase of redox current densities by successive CV

Brought to you by | University of Gothenburg
Authenticated
Download Date | 10/14/17 8:04 AM

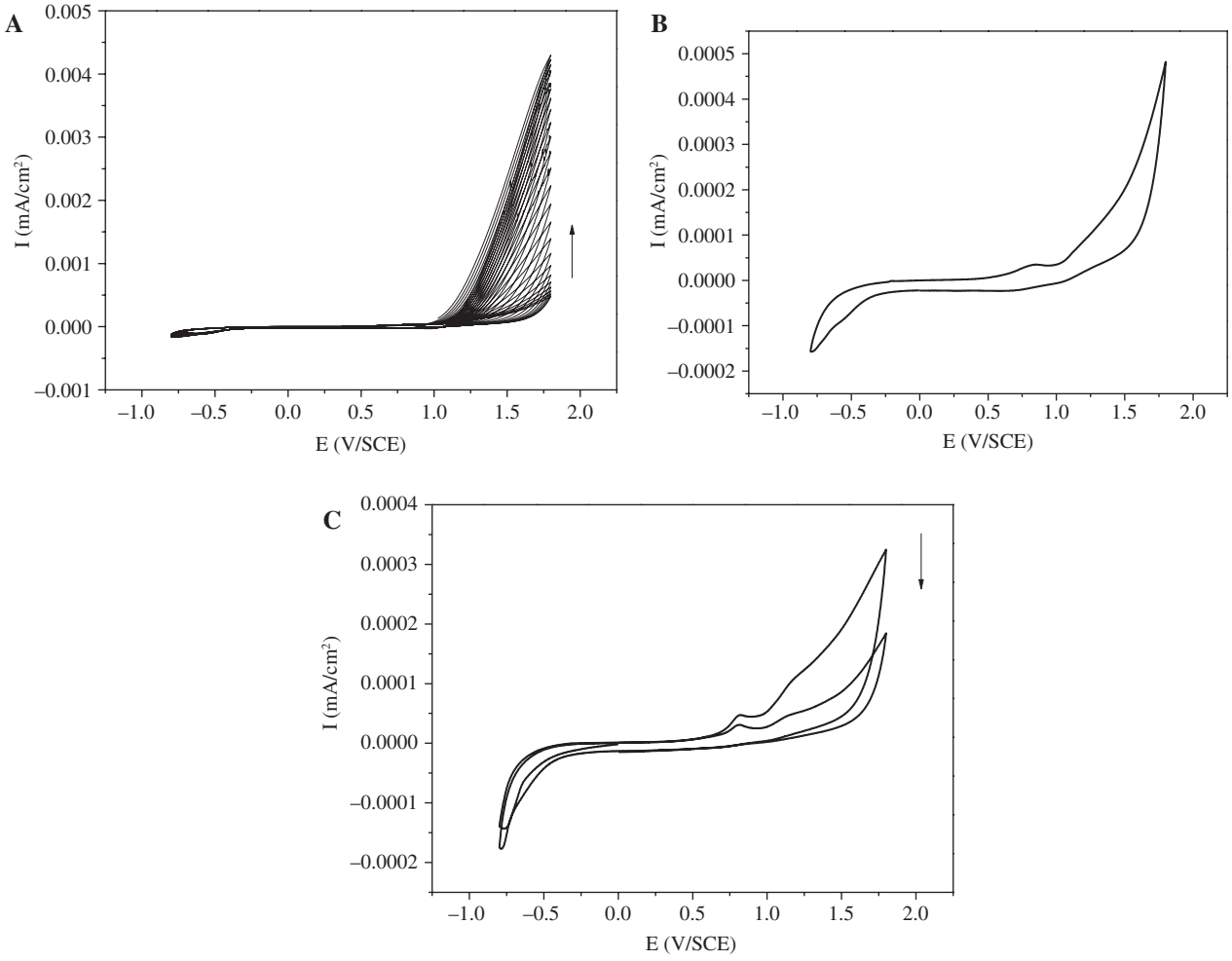

Figure 1: Cyclic voltammograms corresponding to a solution of (NVK) $6 \cdot 10^{-3}$ M dissolved in ($LiClO_4$ 0.1 M/CH_3CN) obtained with v = 10 mV/s, between −0.8 and 1.8 V/SCE, (A) 30 cycling, (B) one cycle, (C) cyclic voltammograms corresponding to poly(N-vinylcarbazole) in ($LiClO_4$ 0.1 M/acetonitrile) solution obtained with v = 10 mV/s, between −0.8 and 1.8 V/SCE, two cycles.

scans showed in Figure 1A indicates the formation of the electrochemically active polymeric film on the electrode surface.

3.2 Cyclic voltamperometry of PVK on ITO electrode

Figure 1C presents the first two CV scans of PVK deposit on ITO. The cyclic voltamperogram revealed the same peaks showing that the PVK polymer formed has the same electrochemical behavior than that observed for the monomer.

We observed during the positive scan potential one peak at $Epa_1 = 0.83$ V/SCE and during the cathodic scan one peak at $Epc_1 = 0.74$ V/SCE. However, contrary to what was observed for the monomer, the current intensity of the oxidation and reduction peaks of the polymer film decreases during the cycling.

3.3 Effect of TiO_2 concentration TiO_2

Figure 2 presents the 21st CV of (NVK) $6 \cdot 10^{-3}$ M dissolved in $LiClO_4$ 0.1 M/CH_3CN, obtained for different contents of TiO_2, at v = 10 mV/s, between −0.8 and 1.8 V/SCE, on an ITO electrode. The recording of cyclic voltammograms shows a redox couple as those not observed in the absence of TiO_2. Thus, there is an irregular appearance and disappearance of oxidation and reduction peak potential.

Figure 2A–D shows the recording of cyclic voltammograms relating to a solution of (NVK) $6 \cdot 10^{-3}$ M dissolved in $LiClO_4$ 0.1 M/CH_3CN, obtained for (A) 0 M TiO_2, (B) $1 \cdot 10^{-2}$ M TiO_2, (C) $3 \cdot 10^{-2}$ M TiO_2, (D) $5 \cdot 10^{-2}$ M TiO_2, recorded at v = 10 mV/s, between −0.8 and 1.8 V/SCE, on an ITO electrode.

When comparing the voltammogram of PVK before and after doping with the semiconductor of TiO_2, a large difference is observed in the form of recorded cyclic

Brought to you by | University of Gothenburg
Authenticated
Download Date | 10/14/17 8:04 AM

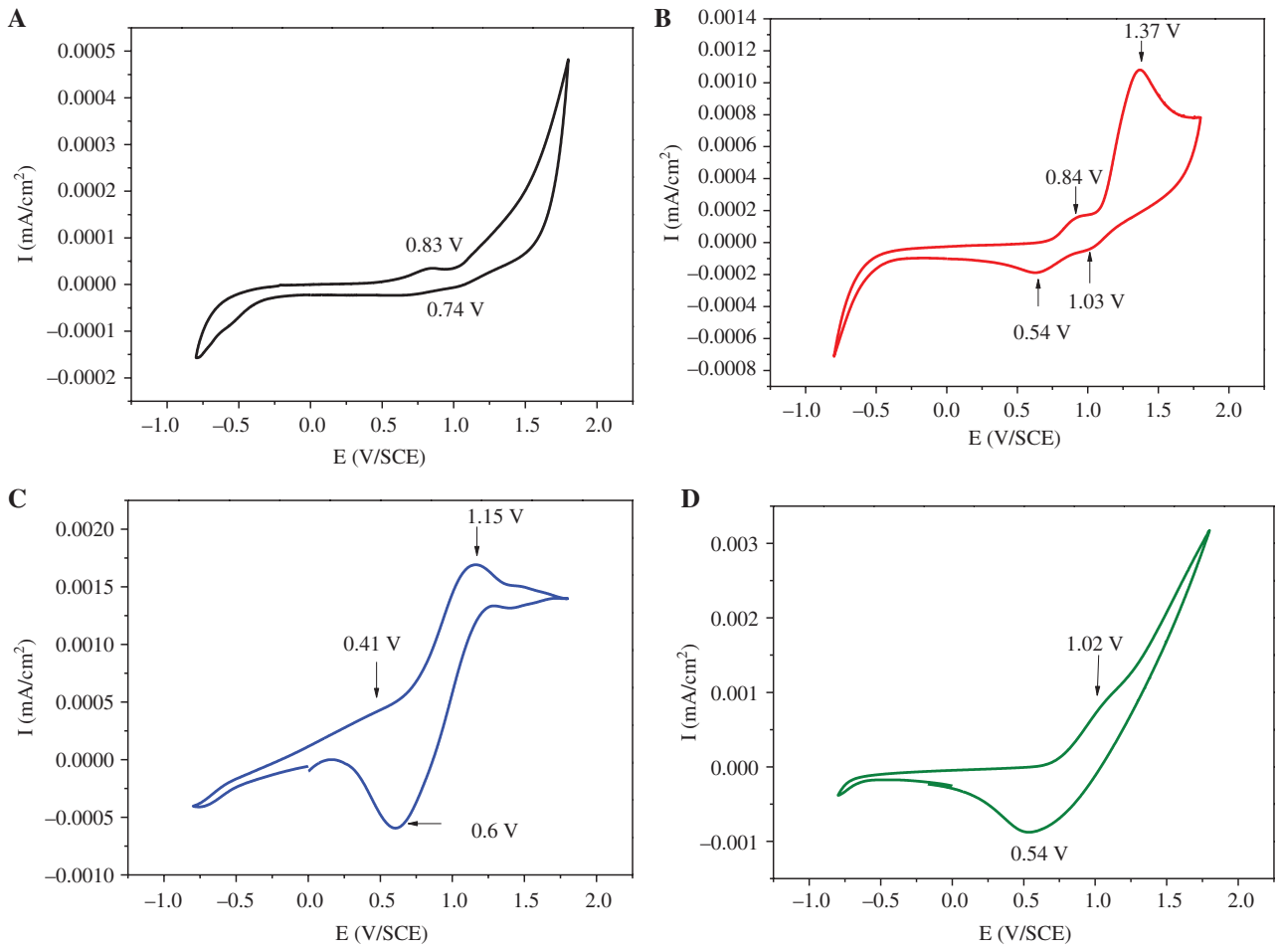

Figure 2: Cyclic voltammograms relating to a solution of (NVK) $6 \cdot 10^{-3}$ M dissolved in $LiClO_4$ 0.1 M/CH_3CN, obtained for (A) 0 M TiO_2, (B) $1 \cdot 10^{-2}$ M TiO_2, (C) $3 \cdot 10^{-2}$ M TiO_2, (D) $5 \cdot 10^{-2}$ M TiO_2 shown in the figure, recorded at v = 10 mV/s, between −0.8 and 1.8 V/SCE, on an ITO electrode.

voltammograms on the ITO electrode of a PVK film doped with TiO_2.

In Figure 2B PVK doped with 10^{-2} M TiO_2, an oxidation reaction developed in the potential range (0.75 V, 1.8 V) (1.37 V wave) during the anode scan. The appearance of two cathode waves located at 0.54 V and 1.03 V confirmed that there is a reaction which develops between the NVK, TiO_2 and $LiClO_4$. Figure 2C represents the voltammogram of PVK/$3 \cdot 10^{-2}$ M TiO_2. Again we observe a change in the cyclic voltammogram pattern by a replacement of the two cathode waves by a large wave localized at 0.6 V. In Figure 2D when PVK doped with 5.10^{-2} M TiO_2, an anode wave was found at 1.02 V and cathode wave was found at 0.54 V were observed. Our result is also very comparable and almost the same phenomenon that happens with that of (10, 25).

Figure 3 shows the cyclic voltammograms relating to a solution of (NVK) $6 \cdot 10^{-3}$ M dissolved in $LiClO_4$ 0.1 M/CH_3CN, obtained for different contents of TiO_2 only recorded at v = 10 mV/s, between −0.8 and 1.8 V/SCE, on a ITO electrode.

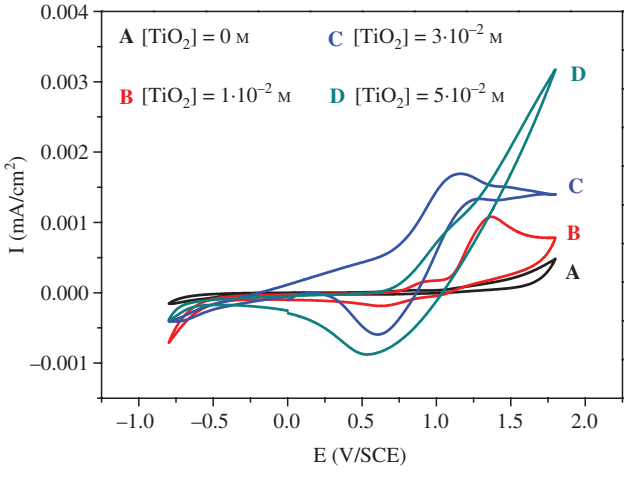

Figure 3: Cyclic voltammograms relating to a solution of (NVK) $6 \cdot 10^{-3}$ M dissolved in $LiClO_4$ 0.1 M/CH_3CN, obtained for different contents of TiO_2 shown in the figure, recorded at v = 10 mV/s, between −0.8 and 1.8 V/SCE, on an ITO electrode.

Brought to you by | University of Gothenburg
Authenticated
Download Date | 10/14/17 8:04 AM

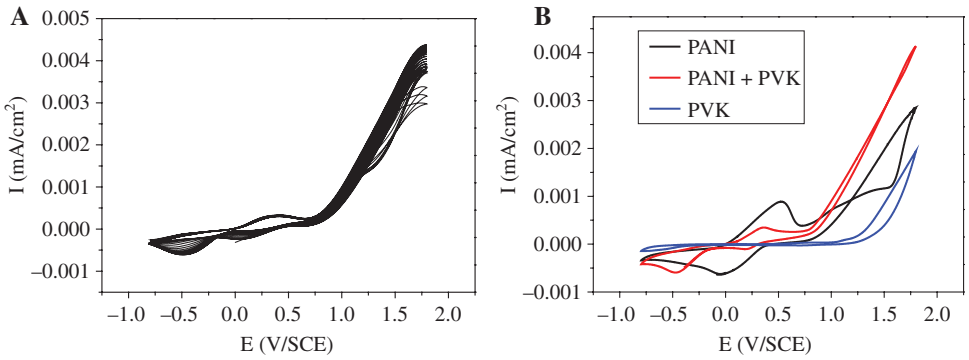

Figure 4: Cyclic voltammograms corresponding to a solution of (NVK) 6.10^{-3} M + (AN) 10^{-1} M dissolved in ($LiClO_4$ 0.1 M/CH_3CN) obtained with v = 10 mV/s, between −0.8 and 1.8 V/SCE, (A) 30 cycling, (B) comparison of cyclic voltammograms corresponding to a solution of (NVK) $6 \cdot 10^{-3}$ M + (AN) 10^{-1} M.

The current intensities of the oxidation and reduction peaks increase with the semiconductor content (TiO_2), and the curves show that the amount of incorporated TiO_2 increases the electro activity of the PVK/ITO electrode. This is likely to result in good contact of the TiO_2 with the PVK, which in turn contributes to a good conductivity of the film.

3.4 Electropolymerization of copolymer in CH_3CN medium

3.4.1 The effect of the aniline addition

The synthesis of the copolymer films was performed electrochemically. Figure 4 shows the CV plot during the electro deposition of the [NVK ($6 \cdot 10^{-3}$ M)/aniline (10^{-1}) M] dissolved in $CH_3CN/LiClO_4$ 0.1 M solution, recorded in a potential range between −0.8 and 1.8 V/SCE, with scan rate v = 10 mV/s on an ITO surface. It is noticed that the shape (intensity, potential and number of redox couple) of the cyclic voltamperogram varies with the addition of aniline. The voltamperograms (Figure 4A) show during the positive scan a potential one anodic peak at $Epa_1 = 0.46$ V/SCE, respectively, and during the cathodic scan two peaks at $Epc_1 = 0.22$ V/SCE and $Epc_2 = 0.41$ V/SCE. These peaks correspond to different oxidation and reduction states of copolymers. In Figure 4B we note that the displacement of the potential peaks is accompanied by an increase in the current intensity of the copolymer compared with PVK and PANI only, which gives us a new copolymer with a better property than that of PVK alone.

3.4.2 Effect of concentration of TiO_2

The superposition of cyclic voltammograms (30 cycles) of the obtained copolymer in a solution of (0.1 M $LiClO_4$ + acetonitrile) in the absence and in the presence of different concentration of TiO_2, on an ITO electrode is shown in Figure 5. The voltammograms were recorded over a potential range of −0.8 to 1.8 V/SCE, at a scanning speed of 10 mV/s. It is noted that the intensity of the peak currents decreases when the semiconductor is added in solution with a concentration of 10^{-2} M and $3 \cdot 10^{-2}$ M of TiO_2 compared to that of the copolymer not doped with TiO_2. At the concentration of $5 \cdot 10^{-2}$ M of TiO_2, the current increased to that of the virgin PVK. This confirms that the addition of TiO_2 at different concentration has no effect on the electrical and electrochemical properties of the copolymer.

3.5 EIS analysis

Figure 6A shows the relative impedance diagrams of an electrode ITO modified by a film of PVK in which the TiO_2

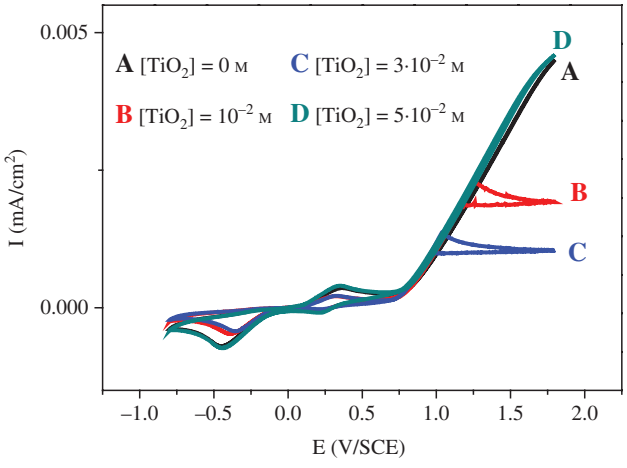

Figure 5: Cyclic voltammograms relating to a solution of (NVK) $6 \cdot 10^{-3}$ M + (AN) 10^{-1} M dissolved in $LiClO_4$ 0.1 M, obtained for different contents of TiO_2, recorded at v = 10 mV/s, between −0.8 and 1.8 V/SCE, on an ITO electrode.

Brought to you by | University of Gothenburg
Authenticated
Download Date | 10/14/17 8:04 AM

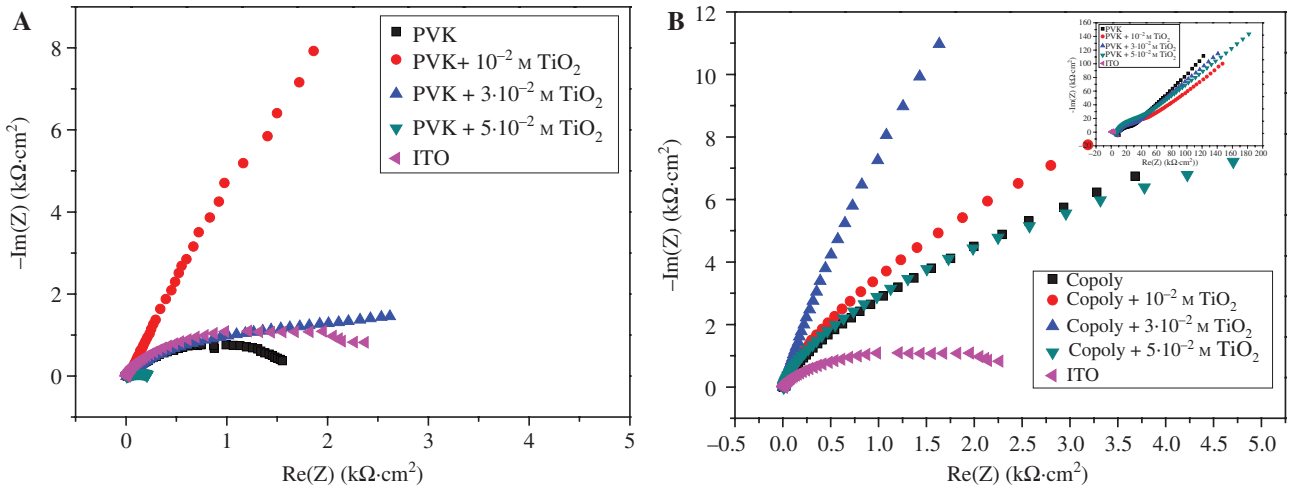

Figure 6: Nyquist diagrams relative to films of (A) (PVK/ITO, PVK/TiO_2/ITO), (B) (copoly/ITO, copoly/TiO_2/ITO).

is incorporated. The films are obtained for different concentrations of TiO_2 0, 10^{-2} M, $3 \cdot 10^{-2}$ M, and $5 \cdot 10^{-2}$ M. The curves were recorded over a frequency range between 50 KHz and 100 MHz, with a 10 mV perturbation. The modified electrode is analyzed in an aqueous solution containing (0.1 M $LiClO_4$ + acetonitrile).

It is clear from this figure that the amplitude of Zr ($k\Omega \cdot cm^2$) varies with concentration of the TiO_2. Nyquist diagrams give a semi-circle that is characteristic of a high-frequency charge transfer process (26).

It is also observed that the diameter of the semi-circle obtained towards the high frequencies decreases with the concentration of TiO_2. The resistance of the composite material is represented by the radius of the semi-circle, the smallest of which is obtained for the doped PVK with $5 \cdot 10^{-2}$ M. Thus, it can be seen that increasing the concentration decreases the radius and consequently increases the conductivity of the film which forms on the electrode. This shows that the electrochemical behavior is governed by the same diffusion process. The presence of TiO_2 in the polymer film affects the electrochemical impedance values and makes the loop more capacitive. The resistance of the electrolyte (R_Ω) and the double layer capacity (C_{dl}) of the composite material PVK/TiO_2 calculated after extrapolation of the Nyquist diagrams are given in Table 1.

Figure 6B shows the Nyquist diagrams corresponding to the copolymer, copolymer/TiO_2 films deposited on ITO in a solution of (0.1 M $LiClO_4$ + acetonitrile) over a frequency range between 50 KHz and 100 mHz. It is observed that the resistivity of the copolymer films increases from 1701 Ω to 2614 Ω with the addition of aniline, thereby dismantling a decrease in conductivity.

Table 1: Electrical parameters corresponding to the PVK films obtained for different concentrations of titanium dioxide.

PVK + TiO_2				
TiO_2 (M)	0	10^{-2}	$3 \cdot 10^{-2}$	$5 \cdot 10^{-2}$
R_Ω (Ω)	1701	–	1346	246
C_{dl}	187	86.65	52.34	250.8

R_Ω (Ω) ITO: 2564.

The Nyquist diagrams in Figure 6B obtained in the presence of TiO_2 show high frequencies characteristic of a charge transfer process.

From the semicircle diameters, the transfer charge resistivity of the copolymer is increased to 10^{-2} M TiO_2 resulting from the decrease in the capacitive effect which becomes less and less important for the films of copolymers modified by incorporation of the semiconductor. Then a decrease in the resistivity is observed with the increase of the TiO_2 concentration and the film becomes more conductive and more capacitive. The corresponding values, given in Table 2, were calculated after extrapolation of the Nyquist plots.

Table 2: Electrical parameters corresponding to the copolymer films obtained for different concentrations of titanium dioxide.

Copolymer + TiO_2				
TiO_2 (M)	0	10^{-2}	$3 \cdot 10^{-2}$	$5 \cdot 10^{-2}$
R_Ω (Ω)	2614	3709	2136	2133
C_{dl}	60.87	42.90	7.33	74.60

Brought to you by | University of Gothenburg
Authenticated
Download Date | 10/14/17 8:04 AM

3.6 Surface morphology of PVK and copolymer films

3.6.1 SEM

From the image of the PVK film in Figure 7A, it is clearly observed that the electrodeposited polymer layer on the ITO substrate is homogeneous. The pure PVK has grains which are well interconnected and adherent.

The darker areas in Figure 7B represent regions with higher atomic numbers which are the conducting polymer in our case. Consequently, the lighter zones identify the areas of TiO_2 which contain pseudo spherical shapes with size distribution in the range of 15–20 nm.

The SEM images corresponding to the ITO plates modified by PVK + $5 \cdot 10^{-2}$ M TiO_2 films are shown in the Figure 7C. It is clear that the particles of the inorganic semiconductor are incorporated into the organic polymer (PVK), thus modifying the morphology, no agglomeration and uniform distribution of the TiO_2 particles in the PVK film. Therefore, we consider that the semiconductor particles can be incorporated into the polymer during NVK electro polymerization which leads to pigmenting of the polymer film, and consequently allows a composite material (PVK/TiO_2) on the electrode. The improvement of the properties of the composite is explained by the fact that PVK and TiO_2 can act as electron donor and acceptor, respectively.

Figure 8A shows SEM micrographs of the copolymer. It is clearly observed that the electrodeposited copolymer layer on the ITO substrate is homogeneous and compact with a spherical shape.

The SEM image in Figure 8B of the copolymer/TiO_2 composite shows that there is no agglomeration of TiO_2 particles in the matrix and that there is a uniform distribution of the TiO_2 and a modification of the copolymer morphology is observed.

3.6.2 AFM

The PVK, PVK/TiO_2 copolymer and copolymer/TiO_2 films were examined by AFM in the contact mode. The effect

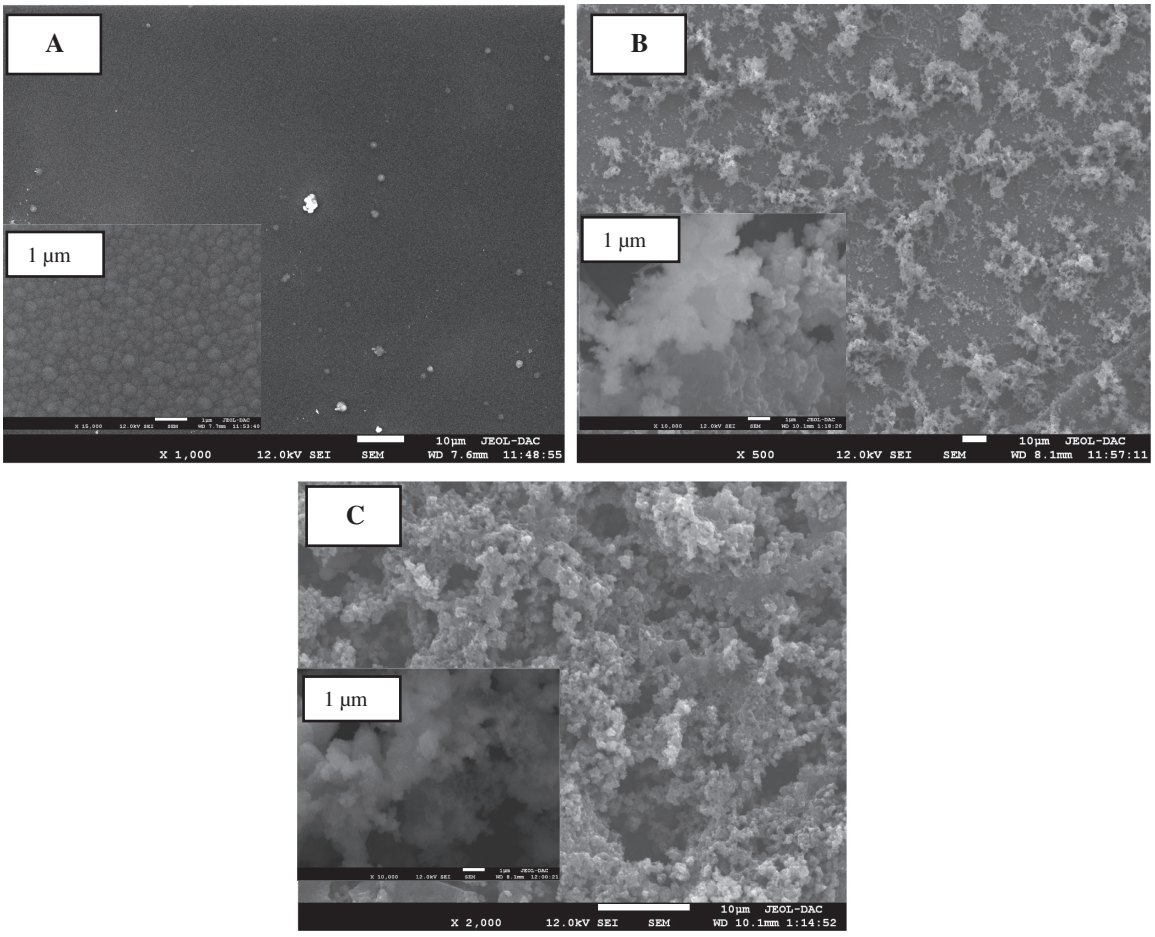

Figure 7: SEM images of (A) PVK/ITO, (B) PVK + ($3 \cdot 10^{-2}$ M) TiO_2/ITO, (C) PVK + ($5 \cdot 10^{-2}$ M) TiO_2/ITO.

Brought to you by | University of Gothenburg
Authenticated
Download Date | 10/14/17 8:04 AM

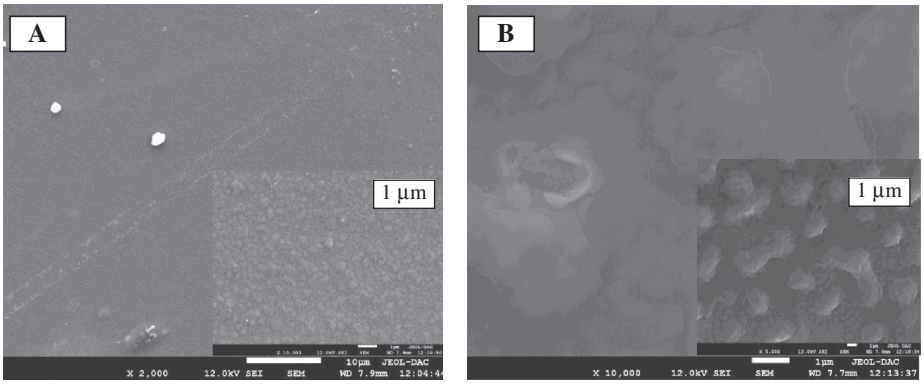

Figure 8: SEM images of (A) copolymer/ITO, (B) copolymer/($3 \cdot 10^{-2}$ M) TiO_2/ITO.

of TiO_2 content on the surface morphology of PVK and copolymer films electrochemically deposited were further evoked by AFM as presented in Figure 9. The result reveals a well-defined grain structure. Moreover, these images show the uniformity and the homogeneity of TiO_2 particles in the surface of each sample. This is confirmed by the SEM. When we compare Figure 9A and B–D, we find that the surface of the PVK film is globular in contrast. The difference between the surface morphologies of PVK and PVK + TiO_2 at different concentrations was clear. The surface is not smooth but contains few voids, compared to the pure PVK film. From these AFM measurements, the root mean square (RMS) surface roughness was calculated for a surface of 20 µm × 20 µm. And the size of the grain (particle) is decreased in proportion to the percentage of TiO_2. This size is finer at $1 \cdot 10^{-2}$ M, which confirms a better distribution of TiO_2 in the copolymer. It is difficult to compare these results with the data in the literature because RMS parameters depend strongly on the scanning length and the thickness of the film.

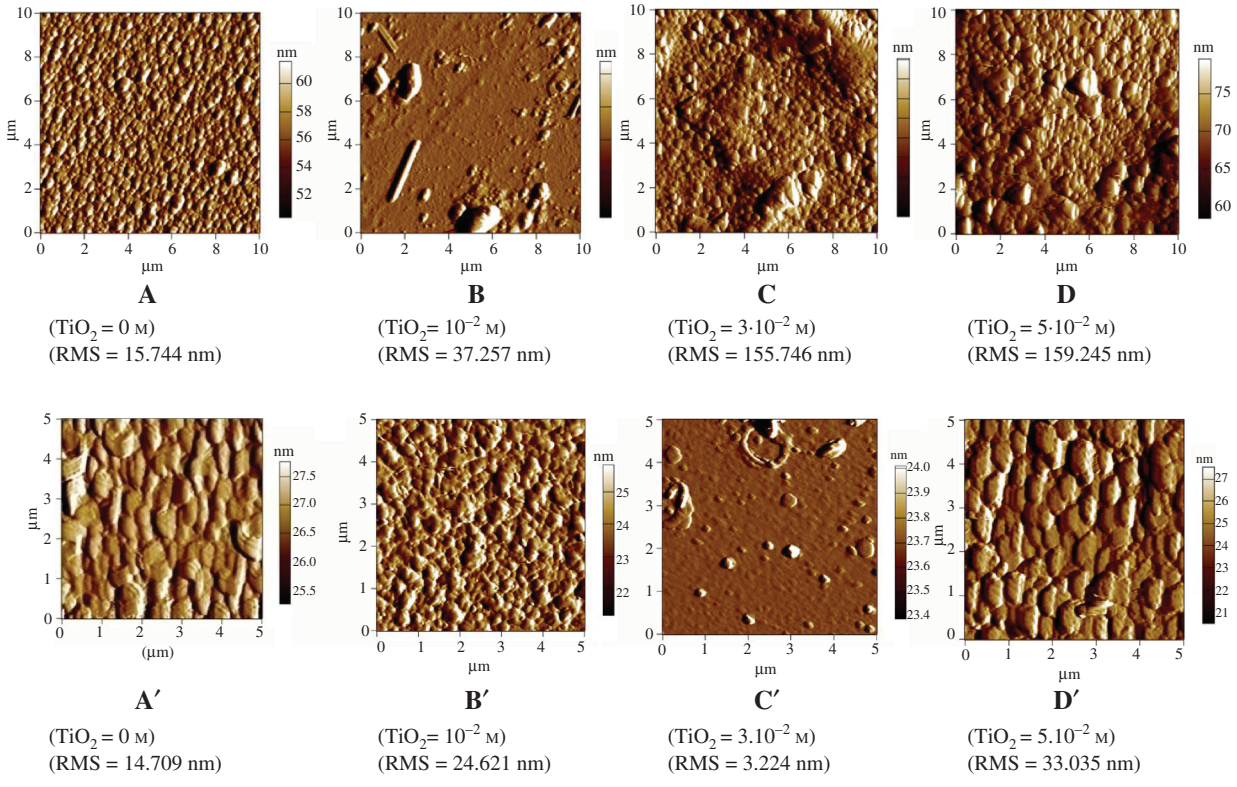

Figure 9: 2D AFM images of (A) PVK, (B) PVK/(10^{-2} M) TiO_2, (C) PVK/($3 \cdot 10^{-2}$ M) TiO_2, PVK/($5 \cdot 10^{-2}$ M) TiO_2. (A′) copoly, (B′) copoly/(10^{-2} M) TiO_2, (C′) copoly/($3 \cdot 10^{-2}$ M) TiO_2, copoly/($5 \cdot 10^{-2}$ M) TiO_2 films electrodeposited on the ITO substrate.

Brought to you by | University of Gothenburg
Authenticated
Download Date | 10/14/17 8:04 AM

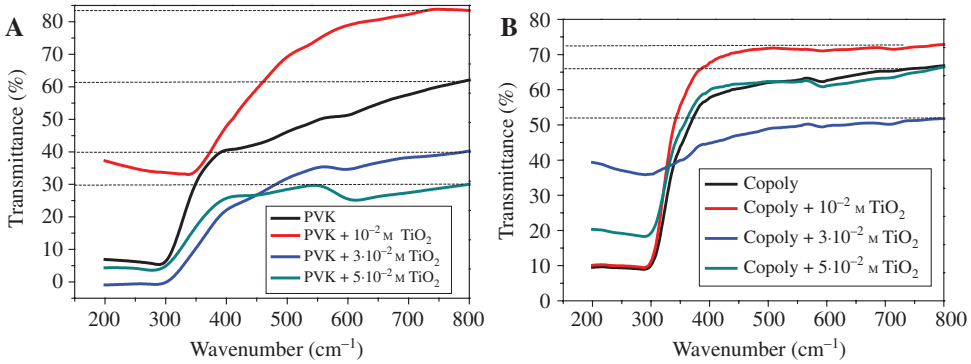

Figure 10: Transmittance spectra of (A) PVK, (B) PVK/TiO_2 thin films electrodeposited at different concentration of TiO_2.

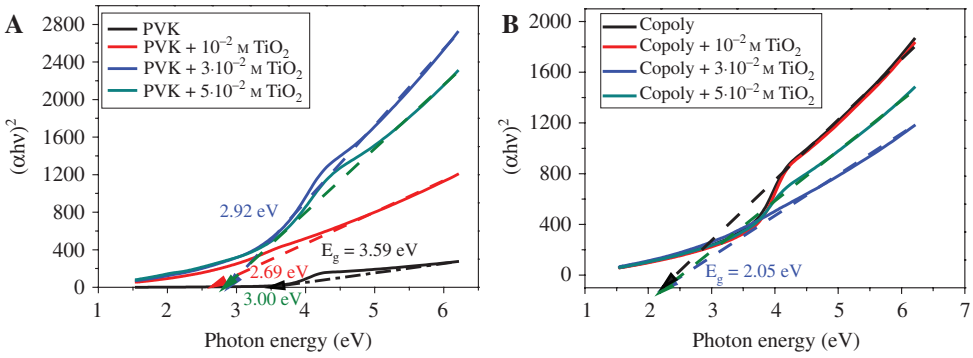

Figure 11: Variation of $(\alpha h\nu)^2$ versus $h\nu$ of (A) PVK, (B) copolymer thin films electrodeposited at different percentage of TiO_2. The inset shows the corresponding variation of the band gap of the samples with TiO_2.

It is clear from the 2D images in Figure 9A′–D′ that the addition of aniline and TiO_2 affects the films topography.

3.7 Absorption measurements

To study the influence of addition of TiO_2 on the optical properties of the PVK thin films, transmittance measurements were conducted and the results are presented in Figure 10A. It was observed that the samples (PVK+10^{-2} TiO_2) exhibited high transmittance (83%) in the visible region, so light can easily pass through it. When light passes, the charge carriers such as holes and electrons are produced proportional to the incident light the photoelectric transducers generate electric current when exposed to light. This confirms that this material can be used in photovoltaic cells. In the case of copolymer shown in Figure 10B which represents the transmittance spectra of copolymer and copolymer/TiO_2 thin films electrodeposited at different concentration of TiO_2, the same phenomenon was observed with no change being made with the addition of PANI.

In order to determine the optical band gap of this material and the type of optical absorption, Tauc (27), Burstein (28) showed that the absorption coefficient and photon energy are related by the following equation:

$$\alpha h\nu = A(h\nu - E_g) \quad [1]$$

In the above equation, A is a constant, E_g is the band gap of the material, α is the absorption coefficient, h the Plank constant, ν is the frequency of the radiation and n has different values depending on the optical absorption process. The corresponded optical band gap energies were estimated from the plot of $(\alpha h\nu)^2$ versus the photon energy ($h\nu$). The band gap was determined by the extrapolating plot. The straight-line portion of the plots shown in Figure 11A indicates the direct transition for all the samples (29). The band gap values of the samples were

Table 3: Values band gap for PVK, PVK/TiO_2.

Sample	Band gap (ev)
PVK	3.59
PVK/TiO_2 (10^{-2} M)	2.69
PVK/TiO_2 ($3 \cdot 10^{-2}$ M)	2.92
PVK/TiO_2 ($5 \cdot 10^{-2}$ M)	3.00

Brought to you by | University of Gothenburg
Authenticated
Download Date | 10/14/17 8:04 AM

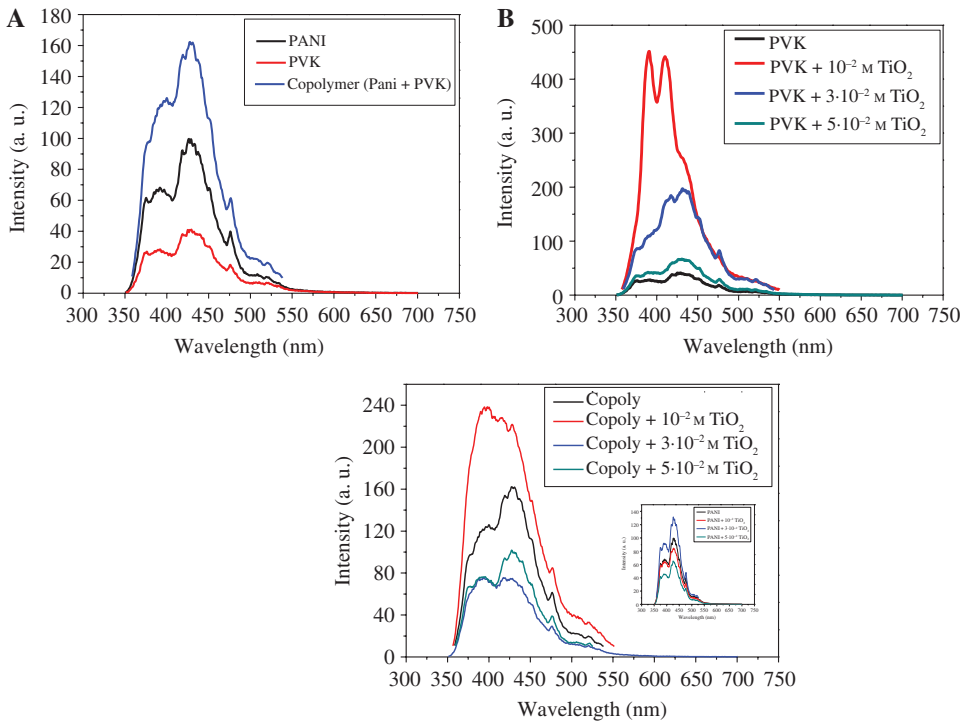

Figure 12: PL spectrum of (A) comparison, (B) PVK, (C) copolymer.

confined between 2.69 and 3.59 eV; they were in good agreement with theoretical band gap value of PVK which is in the range of (3.3–3.5 eV) confirmed in the literature (11, 30).

This curve, Figure 11A, indicates that the optical band gap decreased generally with increasing of concentration of TiO_2 compared with PVK only.

The gap values are reported in Table 3. For the optimal doping at 10^{-2} M, the gap value is 2.69 eV. This is explained by the introduction of the donor levels in the band gap of PVK by the TiO_2, a consequence of an effective doping. In Figure 11B it is evident that the band gaps of the copolymer decrease with the addition of PANI to PVK. But there is no variation in the gap energy with the addition of TiO_2 in the copolymer.

The luminescence spectra were measured on films deposited on ITO substrates, using a Perkin Elmer spectrophotometer. The emission spectra of corresponding PVK, PANI and the copolymer are shown in Figure 12.

The profiles of the PL are recorded for an excitation wavelength of 325 nm. Under this excitation, PVK showed four PL peaks well-marked, respectively (Figure 11A) at

Table 4: Observed absorption peak positions for PVK, PANI, and copolymers.

Sample	Absorption peak position (nm)		
	E_1 (nm)	E_2 [maximum emission (nm)]	E_3 (nm)
PVK	390	427	477
PANI	392	429	476
Copolymer	398	428	476

Table 5: Observed absorption peak positions for PVK, PVK/TiO_2.

Sample	Absorption peak position (nm)		
	E1 (nm)	E2 (nm)	E3 (nm)
PVK	390	427	477
PVK/TiO_2 (10^{-2} M)	391	411	435
PVK/TiO_2 ($3 \cdot 10^{-2}$ M)	409	423	468
PVK/TiO_2 ($5 \cdot 10^{-2}$ M)	393	431	478

Table 6: Observed absorption peak positions for copolymer, copolymer/TiO_2.

Sample	Absorption peak position (nm)		
	E1 (nm)	E2 (nm)	E3 (nm)
Copolymer	398	429	476
Copolymer/TiO_2 (10^{-2} M)	401	412	479
Copolymer/TiO_2 ($3 \cdot 10^{-2}$ M)	392	422	476
Copolymer/TiO_2 ($5 \cdot 10^{-2}$ M)	395	429	476

Brought to you by | University of Gothenburg
Authenticated
Download Date | 10/14/17 8:04 AM

390, 427 477 and 518 nm with a single maximum emission at 427 nm attributed to the transition in the carbazole group of PVK (31).

PANI shows three luminescence peaks at 392, at 429 (maximum emission), at 475, and at 517 nm (Figure 11A), this peaks are originated due to π^*-π transition of the benzoid units, de-excitation from polaron band and bipolaron de-excitation, respectively (32).

The PL of the copolymer is located in the spectral region from 350 to 550 nm with four well-marked bands, respectively, at 398, 429, 476 and at 516 nm as well as bands of lower intensity at 520 and 418 nm. From Figure 11A it is clear that the PL spectrum did not change. While the intensity of the copolymer increases compared with that of the pure PVK and pure PANI. All values are summarized in Table 4.

From Figure 11B it is clear that the PL spectrum did not change when PVK was modified by TiO_2, but the intensity of the PVK/TiO_2 composites was increased by increasing the concentration of TiO_2 relative to that of pure PVK, and the maximum intensity present at 10^{-2} M. The values of absorption peak positions of PVK and PVK/TiO_2 are summarized in Table 5. For the copolymer, the same phenomenon was observed, particularly with an increase in the TiO_2 content, the corresponding intensity of the PL peak increases (Figure 11C, Table 6).

4 Conclusions

The preparation of PVK, (PVK/PANI) copolymer PVK/TiO_2, and copolymer/TiO_2 films by electropolymerization of NVK and aniline was investigated. CV shows anodic and cathodic peaks which are characteristic of the oxidation and the reduction of the formed films. The current intensities of the oxidation and reduction peaks of PVK increase with the semiconductor content (TiO_2). The oxidation and the reduction peak currents increase with the addition of aniline to PVK, which give us a new copolymer with a better property than that of PVK alone. The presence of TiO_2 in the polymer film affects the electrochemical impedance values and makes the loop more capacitive. The morphological analysis of the films surface by AFM and SEM showed that the presence of aniline and TiO_2 modifies the roughness, the electrochemical properties and the morphology of the PVK. The UV-Vis study shows that the samples (PVK+10^{-2} TiO_2) exhibited high transmittance (83%) in the visible region with a band gap of 2.69 eV. There is no variation in the gap energy with the addition of TiO_2 in the copolymer.

References

1. Grazulevicius JV, Strohriegl P, Pielichowski J, Pielichowski K. Carbazole-containing polymers: synthesis, properties and applications. Prog Polym Sci. 2003;28:1297–353.
2. Oh KS, Bae W, Kim H. Dispersion polymerization of N-vinylcarbazole using siloxane-based and fluorine-based surfactants in compressed liquid dimethyl ether. Polymer 2007;48:1450–4.
3. Ates M, Uludag N. Carbazole derivative synthesis and their electropolymerization. J Solid State Electr. 2016;20:2599–612.
4. Martin JL, Bergeson JD, Prigodin VN, Epstein AJ. Magnetoresistance for organic semiconductors: Small molecule, oligomer, conjugated polymer, and non-conjugated polymer. Synthetic Met. 2010;160:291–6.
5. Kulas A, Yi H, Iraqi A. Triarylamine N-functionalized 3,6-linked carbazole main chain polymers and copolymers: preparation and physical properties. J Polym Sci Pol Chem. 2007;45:5957–67.
6. Xuan Y, Pan DC, Zhao NN, Ji XL, Ma DG. White electroluminescence from a poly(N vinylcarbazole) layer doped with CdSe/CdS core-shell quantum dots. Nanotechnology 2006;17:4966–9.
7. Wu W, Li JX, Yang LM, Guo ZX, Dai LM, Zhu DB. The photoconductivity of PVK-carbon nanotube blends. Chem Phys Lett. 2002;364:196–9.
8. Lacaze PC, Dubois JE, desbene-monvernay A. Polymer-modified electrodes as electro chromic material part iii. Formation of poly-N-vinylcarbazole films on transparent semiconductor into surfaces by electropolymerization of NVK in acetonitrile. J Electroanal Chem. 1983;147:107–21.
9. Topart PA, Josowicz M. Study of electrochemically deposited thin poly (N-vinylcarbazole) films. Tolonta. 1994;41:909–16.
10. Baibarac M, Lira-Cantú M, Oró Sol J, Baltog I, Casañ-Pastor N, Gomez-Romero P. Poly (N-vinylcarbazole) and carbon nanotubes based composites and their application to rechargeable lithium batteries. Compos Sci Technol. 2007;67:2556–63.
11. Han Y, Wu G, Chen H, Wang M. Preparation and optoelectronic properties of a novel poly(N-vinylcarbazole) with covalently bonded titanium dioxide. J Appl Polym Sci. 2008;109:882–8.
12. O'Regan B, Gratzel M, Fitzmaurice D. Optical electrochemistry. 2. Real-time spectroscopy of conduction band electrons in a metal oxide semiconductor electrode. J Phys Chem. 1991;95:10528–31.
13. Liang L, Dai S, Hu L, Kong F, Xu W, Wang K. Porosity effects on electron transport in TiO_2 films and its application to dye-sensitized solar cells. J Phys Chem B. 2006;110:12404–9.
14. Lancelle-Beltran E, Prené P, Boscher C, Belleville P, Buvat P, Sanchez C. All-solid-state dye-sensitized nanoporous TiO_2 hybrid solar cells with high energy conversion efficiency. Adv Mater. 2006;18:2579–82.
15. O'Hayre R, Nanu M, Schoonman J, Goossens A, Wang Q, Gratzel M. The influence of TiO_2 particle size in TiO_2/$CuInS_2$ nanocomposite solar cells. Adv Funct Mater. 2006;16:1566–76.
16. Cho B, Kim T-W, Choe M, Wang G, Song S, Lee T. Unipolar nonvolatile memory devices with composites of poly (9-vinylcarbazole) and titanium dioxide nanoparticles. Org Electron. 2009;10:473–7.
17. Ramar A, Saraswathi R, Rajkumar M, Chen SM. Influence of poly (N vinylcarbazole) as a photoanode component in enhancing the performance of a dye sensitized solar cell. J Phys Chem C. 2015;119:23830–8.

Brought to you by | University of Gothenburg
Authenticated
Download Date | 10/14/17 8:04 AM

18. Sonone RS, Raut VM, Murhek GH. Structural and electroluminescence properties of pure PVK and doped TiO_2 polymer thin films. IJARCS. 2014;1:87–94.
19. Muhammad F, Syed K. X-band microwave absorption and dielectric properties of polyaniline-yttrium oxide composites. e-Polymers 2014;14:209–16.
20. Roswani S, Nabilah MKM, Peng CT, Zeinab AJ, Siew CL. Chemical oxidative polymerization of conductive polyaniline-iron oxide composite as an electro-transducer for electrochemical sensing applications. e-Polymers 2016;16:225–33.
21. Yuzhen Li, Yuan Y, Liangzhuan W, Jinfang Z. Processable polyaniline/titania nanocomposites with good photocatalytic and conductivity properties prepared via peroxo-titanium complex catalyzed emulsion polymerization approach. Appl Surf Sci. 2013;273:135–43.
22. Abaci S, Nessark B, Boukherroub R, Lmimouni K. Electrosynthesis and analysis of the electrochemical properties of a composite material: polyaniline + titanium oxide. Thin Solid Films. 2011;519:3596–602.
23. Pawar SG, Patil SL, Chougule MA, Raut BT, Jundale DM, Patil VB. Polyaniline:TiO_2 nanocomposites: synthesis and characterization. Arch Apll Sci Res. 2010;2:194–201.
24. Xia H, Wang Q. Ultrasonic irradiation: a novel approach to prepare conductive polyaniline/nanocrystalline titanium oxide composites. Chem Mater. 2002;14:2158–65.
25. Huang L, Cheng J, Li X, Yuan D, Ni W, Qu G, Guan Q, Zhang Y, Wang B. Sulfur quantum dots wrapped by conductive polymer shell with internal void spaces for high-performance lithium-sulfur batteries. J Mater Chem A. 2015;3:4049–57.
26. Macdonald JR. Impedance spectroscopy and its use in analyzing the steady-state ac response of solid and liquid electrolytes. J Eleciroanal Chem. 1987;223:25–50.
27. Tauc J. In: Abeles F. (ed) Optical properties of solids 22. North Holland Publications, Amsterdam; 1970.
28. Burstein E. Anomalous optical absorption limit in InSb. Phys Rev. 1954;93:632.
29. Belhaj M, Dridi C, Elhouichet H, Jean VC. Study of ZnO nanoparticles based hybrid nanocomposites for optoelectronic Applications. J Appl Phys. 2016;119:095501.
30. Pérez-Gutiérrez E, Percino MJ, Chapela VM, Maldonado JL. Optical and morphological characterization by atomic force microscopy of luminescent 2-styrylpyridine derivative compounds with poly (N-vinylcarbazole) films. Thin Solid Films 2011;519:6015–20.
31. Jiang Y, Zhong G, Chen F. Preparation and optical properties of CdS/PVK nano composites based on CdS nanorod arrays. Adv Mater Res. 2012;391–392:86–9.
32. Ashwini B, Rohom, Priynka UL, Chaure NB. Enhancement of optical absorption by incorporation of plasmonic nanoparticles in PANI films. Nanosci Nanotechnol. 2016;6:83–7.

Brought to you by | University of Gothenburg
Authenticated
Download Date | 10/14/17 8:04 AM

Graphical abstract

Ouahiba Bouriche, Brahim Bouzerafa and Hicham Kouadri

Electrochemical, optical and morphological properties of poly (N-vinylcarbazole/TiO_2) and (N-vinylcarbazole/aniline)/TiO_2 copolymer prepared by electrochemical polymerization

https://doi.org/10.1515/epoly-2017-0105
e-Polymers 2017; x(x): xxx–xxx

Full length article: Poly (N-vinylcarbazole) (PVK) and a new copolymer, PVK/PANI, have been successfully prepared by electrochemical polymerization of N-vinylcarbazole (NVK) and NVK/aniline from acetonitrile medium and $LiClO_4$ supporting electrolyte.

Keywords: composite; cyclic voltammetry; electropolymerization; ITO; NVK; PANI; poly (N-vinylcarbazole); titanium dioxide.

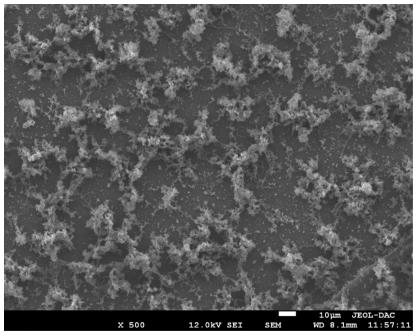

Brought to you by | University of Gothenburg
Authenticated
Download Date | 10/14/17 8:04 AM